Contribution from Ames Laboratory, USDOE, and the Department of Chemistry, Iowa State University, Ames, Iowa 50011

Synthesis, Crystal Structures, and Properties of $LiZn_2Mo_3O_8$, $Zn_3Mo_3O_8$, and $ScZnMo_3O_8$, Reduced Derivatives Containing the Mo_3O_{13} Cluster Unit[1]

C. C. TORARDI and R. E. McCARLEY*

Received April 6, 1984

The new compounds $LiZn_2Mo_3O_8$ (I), $Zn_3Mo_3O_8$ (II), and $ScZnMo_3O_8$ (III) containing the reduced cluster units Mo_3O_{13} have been prepared and characterized by structure determination, magnetic susceptibilities, and infrared spectra. I and II are isomorphous and hexagonal and have space group $R\bar{3}m$, $Z = 6$, with $a = 5.8116$ (6) Å, $c = 31.013$ (8) Å and $a = 5.8617$ (4) Å, $c = 31.100$ (3) Å, respectively. From X-ray powder diffraction data III is hexagonal with $a = 5.8050$ (7) Å, $c = 9.996$ (3) Å, and $Z = 2$ and is isomorphous with $Zn_2Mo_3O_8$. I and III are paramagnetic with moments appropriate for one unpaired electron per cluster. A fit of data for I to the equation $(\chi_M - \chi_{TIP})^{-1} = (T - \Theta)C^{-1}$ over the range 94–300 K gives $\Theta = -350$ (10) K, $C = 0.279$ (5), and $\mu = 1.49$ (2) μ_B. Structure refinements of I and II give Mo–Mo bond distances of 2.578 (1) and 2.580 (2) Å, respectively, for the Mo_3O_{13} cluster units, which may be compared to 2.524 (2) Å in $Zn_2Mo_3O_8$. Changes in the Mo–Mo and Mo–O distances upon reduction of $Zn_2Mo_3O_8$ to I and II are discussed in terms of population of a weakly antibonding MO of a_1 symmetry and the effects of Mo–O π bonding, especially that involving the O atoms bridging the edges of the Mo_3 triangle.

Introduction

Many sulfides, selenides, tellurides, and halides containing discrete metal atom clusters and condensed cluster arrangements are known. A few classic examples of these are $PbMo_6S_8$,[2] Mo_6Cl_{12},[3] Gd_2Cl_3,[4] and ZrCl.[5] However, metal atom clusters and condensed clusters in oxide systems are relatively few in number. Some examples of these oxides are NbO_2,[6] $Mg_3Nb_6O_{11}$,[7] $Ba_{1.14}Mo_8O_{16}$,[8] and $NaMo_4O_6$.[9]

An interesting family of compounds incorporating the Mo_3O_{13} cluster unit includes compounds of the types $A^{II}{}_2Mo_3O_8$ (A = Mg, Mn, Fe, Co, Ni, Zn, Cd)[10] and $LiRMo_3O_8$ (R = Sc, Y, In, Sm, Gd, Tb, Dy, Ho, Er, Yb).[11] The crystal structure of $Zn_2Mo_3O_8$ was determined[12] and shown to consist of a distorted-hexagonal-close-packed arrangement of oxygen atoms (with layer stacking sequence abac) where the oxygen layers are held together by alternating zinc atom layers and molybdenum atom layers. The divalent zinc ions occupy both tetrahedral and octahedral sites in a 1:1 ratio. The tetravalent molybdenum ions occupy octahedral sites to form strongly bonded triangular clusters of molybdenum atoms in which three MoO_6 octahedra are each shared along two edges. Oxygen atoms of the Mo_3O_{13} clusters are shared with other cluster units as represented by the formulation $Mo_3O_4O_{6/2}O_{3/3}$, to give the Mo_3O_8 stoichiometry. A molecular orbital calculation[13] for the Mo_3O_{13} cluster unit explained the strong bonding, weak paramagnetism, and low electrical conductivity of the $A_2Mo_3O_8$ compounds by showing that the six electrons available for Mo–Mo bonding occupy bonding orbitals with all electron spins paired. The basic structure of the $LiRMo_3O_8$ compounds differs from the $A_2Mo_3O_8$ compounds in having a simple oxygen layering of the abab type with the Li^+ ions in tetrahedral sites and the R^{3+} ions in octahedral positions.

The M_3X_{13} cluster unit has also been observed in the halide compounds Nb_3X_8 (X = Cl, Br, I)[14] and Ti_7X_{16} (X = Cl, Br).[15] The first molecular example of a compound containing the M_3X_{13} cluster unit was $W_3(CCH_2C(CH_3)_3)O_3Cr_3(O_2CC(CH_3)_3)_{12}$,[16] where M = tungsten, while the first reported ionic example of an M_3X_{13} cluster was the $W_3O_4F_9{}^{5-}$[17] anion. Ionic species containing the Mo_3O_{13} cluster unit have recently been prepared from aqueous solutions of molybdenum(IV). Two such examples of these ions are $[Mo_3O_4(C_2O_4)_3(H_2O)_3]^{2-}$[18] and $[Mo_3OCl_3(O_2CCH_3)_3(H_2O)_3]^{2+}$.[19]

This paper reports the preparation, crystal structures, and magnetic and physical properties of the new compounds $LiZn_2Mo_3O_8$ and $Zn_3Mo_3O_8$. These phases represent two new types of reduced molybdenum oxides containing Mo_3O_{13} cluster units, $LiA^{II}{}_2Mo_3O_8$ and $A^{II}{}_3Mo_3O_8$. The triangular molybdenum atom cluster units in these new compounds have available seven and eight electrons, respectively, for Mo–Mo bonding. Also described in this paper are the preparation, X-ray powder diffraction data, and magnetic and physical properties of another reduced quaternary oxide of molybdenum, $ScZnMo_3O_8$. This phase represents the first example of an $A^{II}B^{III}Mo_3O_8$ type compound.

Experimental Section

Materials. The starting materials used were Alfa Products Li_2MoO_4 (98.5%), Fisher Certified ACS ZnO, MoO_3, and KOH (85.6%), Atomergic Sc_2O_3 (99.9%), Hach Chemical CsCl (99.9%), Thermo-Electron Mo tubing (99.97%), Rembar Mo sheet (99.95%), Aldrich Mo powder (99.99%), and MoO_2. The Li_2MoO_4 and ZnO were dried at 120 °C before use. Potassium molybdate, which was used as a flux, was prepared by the reaction of KOH with a slight stoichiometric excess of MoO_3 in deionized water. After the solution was filtered, its volume was reduced by heating, and the precipitate was collected on a glass frit, washed with ethanol, dried at 120 °C, and stored over P_4O_{10}. Cesium molybdate, also used as a flux, was prepared by passing an aqueous solution of CsCl through a column of Amberlite IRA-400 strongly basic ion-exchange resin in hydroxide form and neutralizing the effluent with the stoichiometric quantity of MoO_3. The solution was slowly evaporated to dryness and the white solid dried in vacuo at 110 °C for several hours and then stored over P_4O_{10}. Molybdenum dioxide was prepared by two methods: by the reaction of MoO_3 and Mo powder in mole ratio 2:1 in an evacuated fused quartz tube held at 700 °C for 2 days and by the hydrogen reduction of MoO_3 at 460 °C for 48 h. Each preparation of MoO_2 was washed several times with alternate portions of 3 M NH_4OH, deionized water, and 3 M HCl until the washings were colorless and finally dried in vacuo at 110 °C.

Preparation of $LiZn_2Mo_3O_8$. This crystalline compound was first discovered in a multiphase product obtained from a reaction of Li_2MoO_4, ZnO, and MoO_2 in mole ratio 1:2:5. The reactants were ground together

* To whom correspondence should be addressed at Ames Laboratory.

(1) This work was supported by the U.S. Department of Energy through Ames Laboratory, which is operated by Iowa State University under Contract No. W-7405-Eng-82. This research was supported by the Assistant Secretary for Energy Research, Office of Basic Energy Sciences.

(2) Chevrel, R.; Sergent, M.; Prigent, J. *J. Solid State Chem.* **1971**, *3*, 515.
(3) Schafer, H.; von Schnering, H. G.; Tillack, J.; Kuhnen, F.; Wohrle, H.; Baumann, H. *Z. Anorg. Allg. Chem.* **1967**, *353*, 281.
(4) Lokken, D. A.; Corbett, J. D. *Inorg. Chem.* **1973**, *12*, 556.
(5) Adolphson, D. G.; Corbett, J. D. *Inorg. Chem.* **1976**, *15*, 1820.
(6) Marinder, B. O. *Ark. Kemi* **1962**, *19*, 435.
(7) Marinder, B. O. *Chem. Scr.* **1977**, *11*, 97.
(8) Torardi, C. C.; McCarley, R. E. *J. Solid. State Chem.* **1981**, *37*, 393.
(9) Torardi, C. C.; McCarley, R. E. *J. Am. Chem. Soc.* **1979**, *101*, 3963.
(10) McCarroll, W. H.; Katz, L.; Ward, R. *J. Am. Chem. Soc.* **1957**, *79*, 5410.
(11) McCarroll, W. H. *Inorg. Chem.* **1977**, *16*, 3351.
(12) Ansell, G. B.; Katz, L. *Acta Crystallogr.* **1966**, *21*, 482.
(13) Cotton, F. A. *Inorg. Chem.* **1964**, *3*, 1217.
(14) Simon, A.; von Schnering, H. G. *J. Less-Common Met.* **1966**, *11*, 31.
(15) Schafer, H.; Laumanns, R.; Krebs, B.; Henkel, G. *Angew. Chem.* **1979**, *91*, 343.
(16) Katovic, V.; Templeton, J. L.; McCarley, R. E. *J. Am. Chem. Soc.* **1976**, *98*, 5705.
(17) Mattes, R.; Mennemann, K. *Z. Anorg. Allg. Chem.* **1977**, *437*, 175.
(18) Bino, A.; Cotton, F. A.; Dori, Z. *J. Am. Chem. Soc.* **1978**, *100*, 5252.
(19) Bino, A.; Cotton, F. A.; Dori, Z. *Inorg. Chim. Acta* **1979**, *33*, L133.

in a mortar, pelletized under ca. 10000 lb/in.^{2} pressure, sealed in an evacuated molybdenum tube (3 cm length × 1.9 cm diameter), which, in turn, was sealed in an evacuated fused quartz protection tube, and held at 1100 °C for 2 days. Other identified products were unreacted MoO_2 and a new ternary oxide of lithium and molybdenum presently under investigation. Crystals of $LiZn_2Mo_3O_8$ grew as black chunks and thin plates. The composition of this phase was determined from single-crystal and powder X-ray diffraction data as well as chemical analyses (see below).

The compound $LiZn_2Mo_3O_8$ was prepared with 90% purity in powder form by reacting the stoichiometric quantities of Li_2MoO_4, ZnO, MoO_2, and Mo powder as a pellet in a molybdenum tube at 1100 °C for 5 days. The polycrystalline product pellet was powdered in a mortar and washed several times with 3 M HCl and deionized water to remove unreacted ZnO and Li_2MoO_4; the solid was then dried under vacuum at 110 °C. A Guinier X-ray powder diffraction pattern of this product showed only the strongest lines for Mo and MoO_2 and the lines that could be calculated[20] from the single-crystal structure of $LiZn_2Mo_3O_8$. Elemental analyses confirmed a Zn/Li ratio of 2.0 in the mixed-phase product. Combined elemental and oxidation-state analyses for molybdenum suggested a product composition of 89% $LiZn_2Mo_3O_8$, 9.5% MoO_2, and 1.5% Mo.

Preparation of $ScZnMo_3O_8$. It was found that a fluxing agent such as K_2MoO_4 or Cs_2MoO_4 was necessary in the preparation of this compound. Three to five percent by weight of flux was mixed by grinding with the stoichiometric quantities of Sc_2O_3, ZnO, MoO_2, and Mo. The reactant mixture was pelletized, sealed in an evacuated molybdenum tube (3 cm length × 1.3 cm diameter), which, in turn, was sealed in an evacuated inconel protection tube, and fired at 1100 °C for 5–7 days. The product was powdered in a mortar and washed several times with 3 M HCl to remove ZnO and then rinsed with deionized water and dried. A Guinier X-ray powder diffraction pattern, taken on the washed product where K_2MoO_4 flux was used, showed lines of the desired phase, $ScZnMo_3O_8$, lines of the new phase $K_2Mo_{12}O_{19}$,[8] and the strongest lines of Sc_2O_3. The powder pattern of $ScZnMo_3O_8$ is essentially the same as that for $Zn_2Mo_3O_8$ except the unit cell volume is larger for the new compound. If all of the K_2MoO_4 reacted to form $K_2Mo_{12}O_{19}$, then the resultant mixture should contain approximately 80.7% $ScZnMo_3O_8$, 17.2% $K_2Mo_{12}O_{19}$, and 2.1% Sc_2O_3. In contrast, when Cs_2MoO_4 flux was used, the lines of $ScZnMo_3O_8$, $Zn_2Mo_3O_8$, Sc_2O_3, MoO_2 and Mo were all visible in the X-ray diffraction powder pattern.

Preparation of $Zn_3Mo_3O_8$. This phase was first discovered in a reaction product obtained from a mixture of K_2MoO_4, ZnO, and MoO_2 in mole ratio 1:2:5. The reactants were ground in a mortar, pressed into a pellet, sealed in an evacuated molybdenum tube (2.5 cm length × 1.9 cm diameter), which, in turn, was sealed in an evacuated fused quartz tube, and held at 1100 °C for 10 days. Crystals of this new phase grew mostly as bundles of smaller irregularly shaped crystals. Electron microprobe analysis confirmed the presence of Zn and Mo as the only metallic elements in this phase. A Guinier X-ray powder diffraction pattern of these crystals was essentially identical with that of $LiZn_2Mo_3O_8$, except the unit cell volume was larger for $Zn_3Mo_3O_8$. The composition and structure of $Zn_3Mo_3O_8$ were obtained from single-crystal X-ray diffraction data and supported by a magnetic susceptibility measurement, infrared spectra, and physical property observations (see below). Other identified products in the above reaction were $Zn_2Mo_3O_8$[10] and the new compound $K_2Mo_{12}O_{19}$[8] as evidenced from a Guinier X-ray powder diffraction pattern taken on the product pellet.

It was later found that $Zn_3Mo_3O_8$ could be prepared in approximately 97% purity by mixing the stoichiometric quantities of ZnO, MoO_3, and Mo and heating the pelletized reaction mixture in a molybdenum tube at 1100 °C for 5 days (shorter reaction times were not investigated). This product was powdered in a mortar, washed several times with 2 M HCl, rinsed with deionized water, and dried. A Guinier X-ray powder diffraction pattern of this preparation showed only the lines that could be calculated from the structure of $Zn_3Mo_3O_8$ and faintly showed the strongest line for Mo metal.

Preparation of $Zn_2Mo_3O_8$. This compound was prepared as described in the literature[10] by grinding together the stoichiometric quantities of ZnO and MoO_2, pressing the reaction mixture into a pellet, sealing in an evacuated fused quartz tube, and heating at 1100 °C for 4 days. The product was washed with 3 M HCl to remove any ZnO, rinsed with deionized water, and dried.

When finely powdered, $LiZn_2Mo_3O_8$ and $ScZnMo_3O_8$ were black while $Zn_2Mo_3O_8$ was dark green and $Zn_3Mo_3O_8$ was dark brown. All of the new compounds appeared stable toward 3 M hydrochloric acid but, unlike $Zn_2Mo_3O_8$, they were rapidly decomposed in 3 M HNO_3 and slowly decomposed in 1.5 M HNO_3 with gas evolution.

Physical Measurements and Properties. Magnetic susceptibilities of the three compounds $LiZn_2Mo_3O_8$, $ScZnMo_3O_8$, and $Zn_3Mo_3O_8$ were measured by the Gouy method in air at room temperature. Extended measurements of χ vs. T for $LiZnMo_3O_8$ were made on a Faraday balance. The gram susceptibility of $ScZnMo_3O_8$ was corrected for the presence of $K_2Mo_{12}O_{19}$[8] impurity (vide supra), based on an estimate of its weight fraction and χ_g obtained for pure $K_2Mo_{12}O_{19}$. Molar susceptibilities were corrected for diamagnetic core contributions. From room-temperature data the effective magnetic moments per mole formula unit) were calculated from the formula $\mu_{eff} = 2.84(\chi_M'T)^{1/2}$, where χ_M' is the corrected molar susceptibility. Data for $LiZn_2Mo_3O_8$ over the range 95–300 K were fitted to the Curie–Weiss expression $(\chi_M - \chi_{TIP})^{-1} = (T - \Theta)C^{-1}$ to derive values for C and Θ, where $C = N\beta^2\mu^2(3k)^{-1}$. A reasonable estimate of χ_{TIP} for $LiZn_2Mo_3O_8$ was taken as the average value of χ_M' at 298 K, 1.50 × 10^{-4} emu, for $Zn_2Mo_3O_8$ and $Zn_3Mo_3O_8$.

Infrared spectra in the region 300–1000 cm^{-1} were taken with a Beckman IR4250 spectrometer with Nujol mulls of the samples on CsI windows. Spectra were calibrated against the bands of polystyrene. Absorption bands observed for $Zn_2Mo_3O_8$, $ScZnMo_3O_8$, $LiZn_2Mo_3O_8$, $Zn_3Mo_3O_8$, and ZnO are shown in Figure 1, and the absorption frequencies attributed to Mo–O stretching vibrations are listed in Table I.

X-ray Powder Diffraction Data. An Enraf-Nonius Delft triple-focusing Guinier X-ray powder diffraction camera was used with Cu Kα_1 radiation (λ = 1.54056 Å) to obtain unit cell data. National Bureau of Standards silicon powder was mixed with all samples as an internal standard. The lattice parameters for $ScZnMo_3O_8$, $Zn_3Mo_3O_8$, and $Zn_2Mo_3O_8$ were calculated by a least-squares method and are listed in Table II. The compound $ScZnMo_3O_8$ was indexed on the basis of a hexagonal unit cell and $Zn_3Mo_3O_8$ on the basis of an R-centered hexagonal unit cell. The lattice parameters for $Zn_3Mo_3O_8$ were calculated by using the strongest 13 lines and those for $ScZnMo_3O_8$ by using the strongest 14 lines that remained when the lines of known impurities were

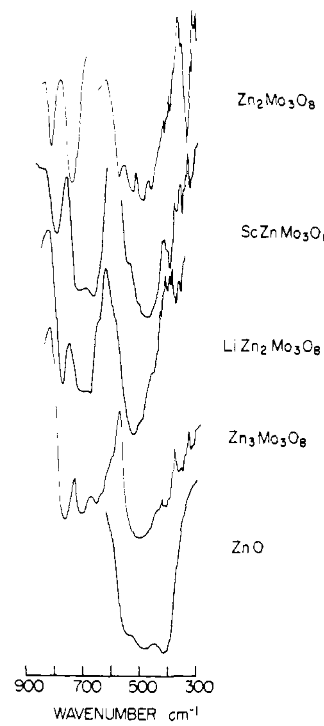

Figure 1. Infrared absorption spectra for Mo_3O_{13} cluster-containing compounds. Mo–O absorptions are in the 600–900-cm^{-1} region. Zn–O absorptions are in the 300–600-cm^{-1} region.

Table I. Infrared Data (cm^{-1}) for Mo–O Absorptions in the 600–900-cm^{-1} Region[a]

$Zn_2Mo_3O_8$	$ScZnMo_3O_8$	$LiZn_2Mo_3O_8$	$Zn_3Mo_3O_8$
817 (m)	790 (m)	767 (s)	760 (s)
742 (s)	712 (s)	695 (s)	700 (s)
725 (m, sh)	660 (s)	670 (s)	650 (s)
		635 (m, sh)	630 (m, sh)

[a] Abbreviations: s = strong; m = medium; sh = shoulder.

(20) Clark, C. M.; Smith, D. K.; Johnson, G. J. "A Fortran IV Program for Calculating X-ray Powder Diffraction Patterns—Version 5"; Department of Geosciences, Pennsylvania State University: State College, PA, 1973.

Table II. Lattice Parameters for Oxide Compounds Containing the Mo_3O_{13} Cluster Unit

compd	*a*, Å	*c*, Å	*V*, Å^3
$LiZn_2Mo_3O_8$	5.8116 (6)	31.013 (8)	3(302.4)[a]
$ScZnMo_3O_8$	5.8050 (7)	9.996 (3)	291.7[b]
$Zn_3Mo_3O_8$	5.8617 (4)	31.100 (3)	3(308.5)[a]
	5.8503 (2)	31.207 (3)	3(308.3)[b]
$Zn_2Mo_3O_8$	5.7742 (3)	9.920 (1)	286.4[b]
	5.759 (4)	9.903 (5)	284.4[c]

[a] From single-crystal X-ray diffraction data. [b] From powder X-ray diffraction data. [c] Reference 12.

Table III. Summary of Crystal Data, Collection and Reduction of Intensity Data, and Refinement of Structures for $LiZn_2Mo_3O_8$ and $Zn_3Mo_3O_8$

	$LiZn_2Mo_3O_8$	$Zn_3Mo_3O_8$
cryst color	black	black
cryst shape	thin plate	thin plate
cryst dimens, mm	0.14 × 0.13 × 0.03	0.22 × 0.22 × 0.12
cryst syst	hexagonal	hexagonal
space group	$R\bar{3}m$	$R\bar{3}m$
cell parameters		
a, Å	5.8116 (6)	5.8617 (4)
c, Å	31.013 (8)	31.100 (3)
V, Å^3	907.2	925.5
Z	6	6
calcd density, g cm^{-3}	6.079	6.588
abs coeff, cm^{-1}	140	160
diffractometer	AL[a]	AL[a]
radiation (graphite monochromated)	Mo Kα	Mo Kα
wavelength, Å	0.710 34	0.710 34
scan type	ω	ω
2θ(max), deg	60	60
abs correcn	ϕ scan[b]	ϕ scan[b]
reflcns measd ($I > 3\sigma_I$)	866	1308
unique reflcns	352	370
no. of parameters	40	40
R^c	0.042	0.060
$R_w{}^d$	0.055	0.080
GOF[e]	2.03	2.66

[a] Ames Laboratory diffractometer described in ref 21. [b] For details see ref 23. [c] The function minimized was $\Sigma w(|F_o| - |F_c|)^2$, where $w = [\sigma(F_o)]^{-2}$. The residual is defined as $R = (\Sigma ||F_o| - |F_c||)(\Sigma |F_o|)^{-1}$. [d] The weighted residual is defined as $R_w = [(\Sigma w |F_o| - |F_c|)^2 (\Sigma w |F_o|)^{-2}]^{1/2}$. [e] The goodness of fit (GOF) is defined as $[\Sigma w(|F_o| - |F_c|)^2 (NO - NV)^{-1}]^{1/2}$, where NO and NV are the number of observations and variables, respectively.

removed. Lattice parameters for $Zn_2Mo_3O_8$ were calculated by using the strongest 18 lines observed in its X-ray powder diffraction pattern.

Collection and Reduction of X-ray Data. Crystals of both compounds were mounted on the tips of glass fibers with epoxy adhesive and used for X-ray data collection. The crystal of $LiZn_2Mo_3O_8$ was indexed as *C*-centered monoclinic on an automated four-circle diffractometer, designed and built at Ames Laboratory,[21] with an automatic indexing program[22] that uses reflections taken from several ω-oscillation photographs as input. During data collection the peak heights of 3 standard reflections that were remeasured every 75 reflections did not show any significant change. Final unit cell parameters and their estimated standard deviations were obtained from the same crystal by a least-squares refinement of 2θ values of 14 Friedel-related pairs of independent reflections randomly distributed in reciprocal space having $2\theta > 30°$. Later examination of the data revealed that $LiZn_2Mo_3O_8$ could be better described in an *R*-centered hexagonal unit cell. Indices in the reduced data set were all converted to rhombohedral equivalents and redundant data averaged to yield 352 reflections satisfying the condition $-h + k + l = 3n$. The 14 reflections originally used to obtain the monoclinic cell parameters were relabeled, and a least-squares fit provided the hexagonal unit cell parameters. Crystal data and further information about data collection and structure refinement are given in Table III. For the crystal of $Zn_3Mo_3O_8$ indexing and data collection proceeded directly with the hexagonal cell. Peak heights of 3 standard reflections remeasured every 75 reflections showed no evidence of decay. Final unit cell parameters were obtained from least-squares refinement of 21 reflections having $2\theta > 24°$. The data for both compounds were corrected for Lorentz, polarization, and background effects, and absorption corrections were applied by use of ϕ-scan data.[23]

Table IV. Positional Parameters for $LiZn_2Mo_3O_8$

atom	position[a]	multiplier	*x*	*y*	*z*
Mo1	18*h*	0.50	0.1856 (2)	0.8144	0.08395 (2)
O1	18*h*	0.50	0.8454 (12)	0.1546	0.0479 (2)
O2	18*h*	0.50	0.4941 (14)	0.5059	0.1247 (2)
O3	6*c*	0.16666	0.00	0.00	0.1174 (3)
O4	6*c*	0.16666	0.00	0.00	0.3704 (3)
Zn1	3*a*	0.037 (1)	0.00	0.00	0.00
Zn2	6*c*	0.097 (1)	0.00	0.00	0.18033 (9)
Zn3	6*c*	0.156 (1)	0.00	0.00	0.30803 (5)
Zn4	6*c*	0.037 (1)	0.00	0.00	0.4873 (2)

[a] Space group $R\bar{3}m$ (No. 166).

Table V. Positional Parameters for $Zn_3Mo_3O_8$

atom	position[a]	multiplier	*x*	*y*	*z*
Mo1	18*h*	0.50	0.1866 (2)	0.8134	0.08351 (3)
O1	18*h*	0.50	0.8469 (20)	0.1531	0.0462 (3)
O2	18*h*	0.50	0.4955 (27)	0.5045	0.1261 (4)
O3	6*c*	0.16666	0.00	0.00	0.1168 (5)
O4	6*c*	0.16666	0.00	0.00	0.3714 (5)
Zn1	3*a*	0.081 (2)	0.00	0.00	0.00
Zn2	6*c*	0.160 (3)	0.00	0.00	0.17968 (9)
Zn3	6*c*	0.163 (2)	0.00	0.00	0.30754 (9)
Zn4	6*c*	0.092 (2)	0.00	0.00	0.4881 (2)

[a] Space group $R\bar{3}m$ (No. 166).

Table VI. Interatomic Distances (Å) for $LiZn_2Mo_3O_8$, $Zn_3Mo_3O_8$, and $Zn_2Mo_3O_8$

	$LiZn_2Mo_3O_8$	$Zn_3Mo_3O_8$	$Zn_2Mo_3O_8$[a]
Mo1–Mo1[b] (2×)	2.578 (1)	2.580 (2)	2.524 (2)
Mo1–Mo1[c] (2×)	3.234 (1)	3.282 (2)	3.235 (2)
Mo1–O1 (6×)	2.063 (6)	2.100 (9)	2.058 (10)
Mo1–O2 (3×)	2.003 (8)	2.056 (13)	1.928 (20)
Mo1–O3 (3×)	2.138 (5)	2.160 (8)	2.128 (30)
Mo1–O4 (1×)	2.079 (7)	2.054 (11)	2.002 (30)
Mo1–O (av)	2.068	2.100	2.040
Zn1–O1 (6×)	2.151 (7)	2.115 (10)	
Zn2–O2 (3×)	1.952 (7)	1.939 (13)	
Zn2–O3 (1×)	1.948 (10)	1.955 (17)	
Zn3–O1 (3×)	1.931 (6)	1.937 (10)	
Zn3–O4 (1×)	1.936 (10)	1.986 (16)	
Zn4–O2 (3×)	1.851 (8)	1.873 (13)	
Zn4–O2 (3×)	2.344 (9)	2.318 (13)	

[a] Reference 12. [b] Intracluster bond distance. [c] Intercluster distance.

Solution and Refinement of the Structures. For $LiZn_2Mo_3O_8$ the Mo positions were located with use of Patterson-superposition techniques.[24] Subsequent least-squares refinement and Fourier electron density maps[25] revealed the Zn and O atom positions. For $Zn_3Mo_3O_8$, the atomic positions located in $LiZn_2Mo_3O_8$ were used as the starting set of positions. In both structures one of the octahedrally coordinated Zn atoms was found to be disordered within its site. Electron density maxima were found along the hexagonal *z* direction just above and below the inversion center located at this site. (Constraining the Zn atom on this $\bar{3}m$ position at 0, 0, $^1/_2$ resulted in a very large isotropic thermal parameter and poor overall refinement with $R = 0.12$.) In $LiZn_2Mo_3O_8$ the Li atoms could not be found from subsequent electron density difference maps and were

(21) Rohrbaugh, W. J.; Jacobson, R. A. *Inorg. Chem.* **1974**, *13*, 2535.
(22) Jacobson, R. A. *J. Appl. Crystallogr.* **1976**, *9*, 115. Lawton, S. L.; Jacobson, R. A. *Inorg. Chem.* **1968**, *7*, 2124.
(23) Karcher, B. A. Ph.D. Disssertation, Iowa State University, Ames, IA, 1981.
(24) Hubbard, C. R.; Babich, M. W.; Jacobson, R. A. "A PL/1 Program System for Generalized Patterson Superpositions", U.S. AEC Report IS-4106; Iowa State University: Ames, IA, 1977.
(25) Powell, D. R.; Jacobson, R. A. "FOUR: A General Crystallographic Fourier Program", U.S. DOE Report IS-4737; Iowa State University: Ames, IA, 1980.

Table VII. Bond Angles (deg) in $LiZn_2Mo_3O_8$ and $Zn_3Mo_3O_8$

	$LiZn_2Mo_3O_8$	$Zn_3Mo_3O_8$
Mo1-Mo1-Mo1	60.00	60.00
Mo1-C2-Mo1	80.1 (3)	77.7 (4)
Mo1-O4-Mo1	76.6 (3)	77.8 (5)
O1-Mo1-O1	81.6 (2)	79.7 (3)
O1-Mo1-O2	93.8 (3)	94.8 (4)
O1-Mo1-O2	167.8 (3)	166.6 (5)
O1-Mo1-O3	78.6 (2)	78.4 (3)
O1-Mo1-O4	90.0 (2)	90.3 (3)
O2-Mo1-O2	88.5 (2)	87.8 (4)
O2-Mo1-O3	89.5 (5)	88.6 (9)
O2-Mo1-O4	101.3 (3)	102.0 (5)
O3-Mo1-O4	164.8 (3)	165.2 (5)
O4-Mo1-Mo1	51.7 (2)	51.1 (3)

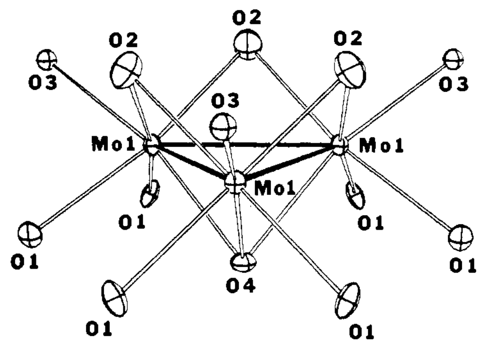

Figure 2. The Mo_3O_{13} cluster unit as found in the compounds $LiZn_2Mo_3O_8$, $Zn_3Mo_3O_8$, and $Zn_2Mo_3O_8$.

assumed to be partially occupied in the same sites that are partially occupied in Zn atoms. Full-matrix least-squares refinement[26] on all positional and anisotropic thermal parameters, as well as all Zn occupation numbers (multipliers), was then conducted. The final electron density difference maps were flat to ≤ 1 e/Å^3. The atomic scattering factors used were those of Hanson et al.[27] for neutral atoms; Mo and Zn were corrected for the real and imaginary parts of anomalous dispersion.[28]

Results and Discussion

Crystal Structures of $LiZn_2Mo_3O_8$ and $Zn_3Mo_3O_8$. Final positional parameters for $LiZn_2Mo_3O_8$ and $Zn_3Mo_3O_8$ are listed in Tables IV and V, respectively. Important interatomic distances for both compounds are given in Table VI, and bond angles for both compounds are listed in Table VII. Observed and calculated structure factors, atomic thermal parameters, and X-ray powder diffraction data are available as supplementary material.

The essential structural features of $LiZn_2Mo_3O_8$ (I) and $Zn_3Mo_3O_8$ (II) are the same and are related to those of $Zn_2Mo_3O_8$.[12] Both new compounds consist of a distorted cubic close packing (abc) of oxygen atoms in which the oxygen layers are held together by alternate layers of zinc and molybdenum ions. The zinc ion sites in $LiZn_2Mo_3O_8$ are fractionally occupied with roughly one-fourth of the zinc ions in approximately octahedral coordination with oxygen and three-fourths in approximately tetrahedral coordination with oxygen. When the sites are not occupied by zinc ions, they are assumed to contain the lithium ions and result in the formulation $Li^{o}_{0.56}Li^{t}_{0.48}Zn^{o}_{0.44}Zn^{t}_{1.52}Mo_3O_8$ (this assumes the X-ray scattering power of Li^+ to be negligible and to have no affect on the zinc ion occupation numbers). The same zinc ion sites are fully occupied in $Zn_3Mo_3O_8$ with one-third of the zinc ions in approximately octahedral coordination with oxygen and two-thirds in approximately tetrahedral coordination with oxygen, thus resulting in the formulation $Zn^{o}_{1}Zn^{t}_{2}Mo_3O_8$. Within the molybdenum layers of both compounds, the ions are arranged with threefold symmetry to form an equilateral triangular pattern of bonded (and nonbonded) Mo atoms each in approximately octahedral coordination with oxygen with the octahedra sharing edges.

Each trimeric molybdenum atom cluster is bonded to a total of 13 oxygen atoms as shown by the ORTEP drawing in Figure 2. The solid, black lines in this figure represent Mo–Mo bonding, and the unfilled lines represent Mo–O bonding, while the atomic labels correspond to those in tables VI and VII. Each Mo atom in the cluster is bonded to two other molybdenum atoms and six oxygen atoms. The Mo_3O_{13} cluster unit contains one oxygen atom (O4) that is triply bridging to the three Mo atoms in a trigonal-pyramidal fashion and has three oxygen atoms (O2) that are each doubly bridging to two Mo atoms along the three edges of the triangle. Each molybdenum atom in the cluster is also bonded to three terminal oxygen atoms (O1 and O3). These terminally bonded oxygen atoms also connect individual clusters to six other surrounding clusters in a hexagonal-like pattern. Oxygen atoms O1 are each shared between two triangular cluster units while oxygen atoms O3 are each shared between three separate cluster units, resulting in the connectivity formula $[Mo_3O_{1/1}O_{3/1}O_{6/2}O_{3/3}]$

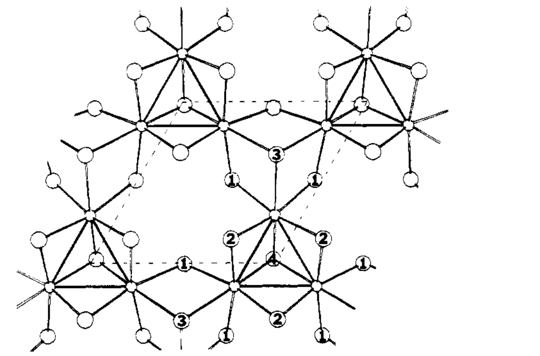

Figure 3. View down the *c* axis of $LiZn_2Mo_3O_8$ and $Zn_3Mo_3O_8$ showing an O–Mo–O section and the connectivity between Mo_3O_{13} cluster units, $Mo_3O_{1/1}O_{3/1}O_{6/2}O_{3/3}$.

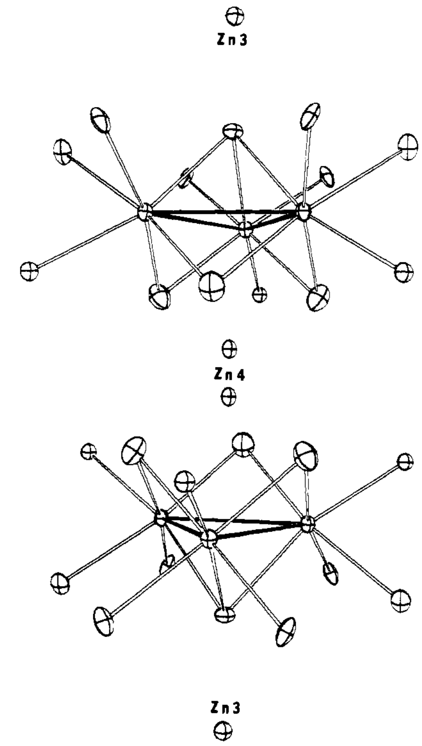

Figure 4. View perpendicular to the *c* axis of $LiZn_2Mo_3O_8$ and $Zn_3Mo_3O_8$ showing the arrangement of two Mo_3O_{13} clusters and the disordered-octahedral zinc ion (Zn4) site.

(26) Lapp, R. L.; Jacobson, R. A. "ALLS, A Generalized Crystallographic Least Squares Program", U.S. DOE Report IS-4708; Iowa State University: Ames, IA, 1979.
(27) Hanson, H. P.; Herman, F.; Lea, J. D.; Skillman, S. *Acta Crystallogr.* **1964**, *17*, 1040.
(28) Templeton, D. H. In "International Tables for X-ray Crystallography", 1st ed.; Macgillavry, C. H., Rieck, G. D., Eds.; Kynoch Press: Birmingham, England, 1962; Vol. III, p 215.

Table VIII. Magnetic Data for Oxide Compounds Containing the Mo_3O_{13} Cluster Unit

compd	$10^4\chi_M'$, cgsu	μ_{eff}, μ_B	compd	$10^4\chi_M'$, cgsu	μ_{eff}, μ_B
$Zn_2Mo_3O_8$[a]	1.4	0.6	$LiZn_2Mo_3O_8$	5.5	1.2
$ScZnMo_3O_8$	8.7	1.5	$Zn_3Mo_3O_8$	1.6	0.6

[a] Reference 10.

= Mo_3O_8, as shown in Figure 3. All atoms in the unit cells for both compounds I and II lie in mirror planes.

Within the Mo_3O_{13} clusters, the molybdenum ions are strongly bonded to one another with bond distances of 2.578 (1) Å (I) and 2.580 (2) Å (II), which are ca. 0.15 Å shorter than the distance between nearest neighbors in bccub molybdenum metal. The next nearest Mo–Mo interatomic distances of 3.234 (1) Å (I) and 3.282 (2) Å (II) indicate no metal–metal-bonding interaction between trimeric cluster units. Each triply bridging oxygen atom (O4) with Mo–O distances of 2.079 (7) Å (I) and 2.054 (11) Å (II) is also coordinated to tetrahedral zinc (Zn3). The doubly bridging oxygen atoms (O2) are each strongly bonded to two molybdenum atoms with Mo–O distances of 2.003 (8) Å (I) and 2.056 (13) Å (II) and are also coordinated to tetrahedral zinc (Zn2) and octahedral zinc (Zn4). The longest Mo–O bond lengths are those involving oxygen atoms (O3): 2.138 (5) Å for compound (I) and 2.160 (8) Å for compound (II). These terminal oxygen atoms are also coordinated to tetrahedral zinc (Zn2). Terminal oxygen atoms (O1) are bonded to molybdenum with bond distances of 2.036 (6) Å (I) and 2.100 (9) Å (II) and also form octahedral interstices for zinc ions (Zn1).

The oxygen atom layers are distorted from a closest packing arrangement in both $LiZn_2Mo_3O_8$ and $Zn_3Mo_3O_8$. The intralayer O–O distances range from 2.70 to 3.12 and 2.69 to 3.17 Å for compounds (I) and (II), respectively. The average interlayer O–O spacing is shorter between O–Mo–O sections, 2.41 Å (I) and 2.47 Å (II), than between O–Zn–O sections, 2.76 Å (I) and 2.71 Å (II).

Discussion of the $LiZn_2Mo_3O_8$ and $Zn_3Mo_3O_8$ Compounds. The crystal structure refinement of $LiZn_2Mo_3O_8$ has established the Zn, Mo, and O stoichiometry, while chemical analyses have shown the Zn/Li ratio to be 2.0. Evidence for the presence of lithium in this phase also comes from X-ray powder diffraction data obtained on the chemically analyzed preparations. The only lines present in these powder patterns are the same lines that can be calculated[20] from the trigonal structure of $LiZn_2Mo_3O_8$ and the strongest lines of Mo and MoO_2. If the Li^+ ions were to reside in the partially occupied zinc ion sites when zinc was absent from these sites, then the $LiZn_2Mo_3O_8$ stoichiometry would result. This occupation scheme appears most likely for several reasons. One reason is that both zinc and lithium ions are known to occupy either octahedral or tetrahedral oxygen interstices. Another reason is that the ionic radii for Zn^{2+} and Li^+ are almost identical,[29] with 0.74 vs. 0.76 Å for octahedral and 0.60 vs. 0.59 Å for tetrahedral Zn^{2+} and Li^+ ions, respectively. Further support for this Zn–Li occupation model comes from the crystal structure of $Zn_3Mo_3O_8$. The zinc ions in $Zn_3Mo_3O_8$ fully occupy the same octahedral and tetrahedral sites that are only partially occupied by zinc ions in $LiZn_2Mo_3O_8$ (i.e. additional zinc ions do not occupy any "new" sites in $Zn_3Mo_3O_8$).

Magnetic susceptibility measurements for $LiZn_2Mo_3O_8$ and $Zn_3Mo_3O_8$ support the structures of these two compounds. The molybdenum ions in $LiZn_2Mo_3O_8$ are in the net oxidation state of +3.66, so there are seven electrons available per trinuclear cluster unit for metal–metal bonding. Six of these electrons are known to reside in bonding orbitals[13] with their spins paired, therefore leaving one unpaired electron. The observed room-temperature magnetic moment of 1.2 μ_B for $LiZn_2Mo_3O_8$ (Table VIII) is consistent with this assessment. The Mo ions in $Zn_3Mo_3O_8$ are in the +3.33 net oxidation state, and there are eight electrons available per molybdenum trimer for Mo–Mo bonding. Once again, six of these eight electrons reside in bonding orbitals with their spins paired, and according to a molecular orbital calculation,[13] the next two electrons should occupy an a_1 orbital (C_{3v} symmetry) with their spins paired. The observed small magnetic moment of 0.6 μ_B for $Zn_3Mo_3O_8$ (Table VIII), about the same as that for $Zn_2Mo_3O_4$, supplies evidence for this spin-paired electron occupation scheme. The weak magnetic moments observed for these last two materials most likely arise from a temperature-independent paramagnetic (TIP) contribution to the susceptibility.

A more detailed picture of the magnetic properties of $LiZn_2Mo_3O_8$ is provided by the χ_M' vs. T data over the range 94–300 K. From least-squares fitting of data at 33 temperatures the values $C = 0.279$ (5), $\mu = 1.49$ (2) μ_B, and $\Theta = -350$ (10) K were derived. The large value of Θ indicates strong antiferromagnetic coupling between cluster units and is responsible for the low value of μ_{eff} (1.2 μ_B) observed at room temperature (Table VIII). Although the magnetic moment of 1.49 μ_B is somewhat low, it does confirm that the clusters in this compound contain the expected one unpaired electron, consistent with a $^2A_1$ ground state.

It has also been observed that the metal–metal and metal–oxygen bond distances in these trinuclear cluster compounds become longer as the oxidation state of molybdenum is lowered. Table VI compares the Mo–Mo and Mo–O bond lengths for the compounds $Zn_2Mo_3O_8$, $LiZn_2Mo_3O_8$, and $Zn_3Mo_3O_8$. The increase in Mo–Mo bond lengths is attributed to Mo–O π-bonding effects and is discussed below. The increase in Mo–O bond distances arises from the placement of more electron density on the molybdenum ions. This weakening of Mo–O interactions is also manifested in the interlayer oxygen spacings of the new compounds. As the Mo–O interactions become weaker, the interlayer oxygen distance in the O–Mo–O layers becomes longer while in the O–Zn–O layers the oxygen interlayer spacing becomes shorter. As expected, these effects are also evident in the Mo–O infrared absorption bands for these compounds, which shift to relatively lower energies as the triangular clusters are reduced. Figure 1 shows the IR absorption spectra for these compounds, and Table I lists the observed band energies assigned to Mo–O absorptions. The bands in the region 300–600 cm^{-1} are attributed to Zn–O absorptions as seen for the compound ZnO. Although ZnO contains only tetrahedrally coordinated Zn ions, octahedral Zn–O bonds would be expected to absorb radiation of lower energies. The 2% increase in unit cell volume for $Zn_3Mo_3O_8$, relative to the volume of $LiZn_2Mo_3O_8$, thus results from the increase in the molybdenum–molybdenum and molybdenum–oxygen bond distances.

Structure and Discussion of $ScZnMo_3O_8$. On the basis of X-ray powder diffraction data, the structure of $ScZnMo_3O_8$ is essentially identical with that of hexagonal $Zn_2Mo_3O_8$ (space group $P6_3mc$).[12] The 2% increase in unit cell volume for $ScZnMo_3O_8$ is attributed to longer Mo–Mo and Mo–O bond distances arising from a one-electron reduction of the Mo_3O_{13} clusters that are present in $Zn_2Mo_3O_8$. The Sc^{3+} ions are assumed to occupy the octahedral sites while the Zn^{2+} ions occupy the tetrahedral sites. Ionic radii for trivalent scandium and divalent zinc ions in octahedral oxygen coordination are almost identical,[29] 0.745 Å for Sc^{3+} and 0.74 Å for Zn^{2+}. Therefore, it is assumed that the presence of Sc^{3+} ions in the octahedral sites has negligible effect on the change in unit cell volume when $Zn_2Mo_3O_8$ and $ScZnMo_{O8}$ are compared. A comparison of the Mo–O infrared absorption energies for these two compounds (Figure 1 and Table I) reflects the longer Mo–O bond lengths in $ScZnMo_3O_8$.

Magnetic susceptibility data for this new compound supplies evidence that the Mo_3O_{13} clusters each possess seven electrons for metal–metal bonding. The effective magnetic moments of 1.5 μ_B confirms the presence of one unpaired electron in each trinuclear cluster unit as expected for the stoichiometry $ScZnMo_3O_8$. The much greater reactivity of this new compound toward oxidation in dilute nitric acid solutions, relative to that of $Zn_2Mo_3O_8$, also supports the assessment of $ScZnMo_3O_8$ as a more reduced phase.

(29) Shannon, R. D. *Acta Crystallogr., Sect. A: Cryst. Phys., Diffr., Theor. Gen. Crystallogr.* **1976**, *A32*, 751.

Conclusions

The new compounds $LiZn_2Mo_3O_8$, $ScZnMo_3O_8$, and $Zn_3Mo_3O_8$ are three new important members in the family of reduced molybdenum oxides containing the Mo_3O_{13} cluster unit. The metal orbitals in these trinuclear molybdenum atom clusters are now known to accommodate six, seven, and eight electrons in the compounds $Zn_2Mo_3O_2$, $LiZn_2Mo_3O_8/ScZnMo_3O_8$, and $Zn_3Mo_3O_8$, respectively. The individual Mo_3O_{13} clusters in $Zn_2Mo_3O_8$, which possess $3m$ (C_{3v}) symmetry, were treated by an LCAO–MO method and Huckel-type calculations were carried out.[13] Two d orbitals per molybdenum atom were reserved for Mo–O bonding, and the three remaining d orbitals were used for metal–metal interactions. The energy level diagram that emerged from this calculation provided three bonding orbitals (a_1 and e), an approximately nonbonding level (a_1), and five antibonding orbitals (2e and a_2). This energy level scheme explained the weak paramagnetism (Table I), low electrical conductivity, and short Mo–Mo bond distance of 2.524 (2) Å in $Zn_2Mo_3O_8$. Each molybdenum atom, with formal oxidation state of +4, would contribute two electrons to the orbitals of the cluster. These six electrons fill the strongly bonding a_1 and e molecular orbitals. According to this molecular orbital picture, a seventh electron (as in $LiZn_2Mo_3O_8$) would occupy a relatively nonbonding orbital. However, the observed Mo–Mo bond distance of 2.578 (1) Å in $LiZn_2Mo_3O_8$ is 0.054 Å longer than that Mo–Mo bond distance in $Zn_2Mo_3O_8$, indicative of an antibonding effect.

More recent MO calculation of $[Mo_3O_4]^{4+}$ and $[Mo_3O_4(OH)_6(H_2O)_3]^{2-}$ as models for the six-electron Mo_3O_{13} cluster units[30] indicate that the Mo–Mo bonding interactions are influenced strongly by interactions with the capping and edge-bridging ligand atoms of the $[Mo_3O_4]^{4+}$ core. Binding of the remaining peripheral ligands, as in $[Mo_3O_4(OH)_6(H_2O)_3]^{2-}$, has only minor influence on the Mo–Mo bonding. Calculations also were made for the core $[Mo_3OCl_3]^{5+}$ containing eight electrons for the metal–metal interactions.[30] This cluster core is present in the ion $[Mo_3OCl_3(O_2CCH_3)_3(H_2O)_3]^{2+}$, for which the Mo–Mo bond distance of 2.550 (2) Å was reported.[19] This distance is longer than the Mo–Mo bond distances of 2.486 and 2.524 Å reported for the six-electron clusters in $[Mo_3O_4(C_2O_4)_3(H_2O)_3]^{2-}$[18] and $Zn_2Mo_3O_8$, respectively. The Mo–Mo distances 2.578 and 2.580 Å, respectively, for the seven- and eight-electron clusters in $LiZn_2Mo_3O_8$ and $Zn_3Mo_3O_8$ thus provide consistent evidence for a slight lengthening of the Mo–Mo bonds with reduction of the six-electron cluster units. It is surprising that the Mo–Mo bonds in $Zn_3Mo_3O_8$ are longer than those in $[Mo_3OCl_3(O_2CCH_3)_3(H_2O)_3]^{2+}$, even though the latter has the larger edge-bridging atoms (Cl), which would be expected to promote somewhat longer bonds. Bursten et al.[30] suggest that the increased bond distance in the eight-electron clusters might arise either from a greater effective atomic radius for Mo upon reduction from +4 to $+3^1/_3$ or from increased electron donation from the ligands into an orbital that is weakly antibonding with reference to the canonical orbitals of Mo_3^{10+}. The change in coordination about the edge-bridging O atoms O2 and the concurrent rehybridization of the atomic orbitals on these atoms upon reduction from $Zn_2Mo_3O_8$ to $LiZn_2Mo_3O_8$ or $Zn_3Mo_3O_8$ does not aid in reaching a clear interpretation of these effects. However, it does appear that strong π interactions in the Mo–O edge-bridging bonds will favor stronger antibonding character in the LUMO of the $[Mo_3O_4]^{4+}$ unit. Evidence for Mo–O π bonding comes from an examination of Mo–O bond lengths in the Mo_3O_{13} clusters. It has been observed that the shortest Mo–O bond distances in these compounds are those involving the doubly bridging O atoms, O2 in Figure 2 and Table VI. These O atoms in $Zn_2Mo_3O_8$ are each bonded to two Mo atoms and one Zn ion in an sp^2-like planar arrangement (the sum of the Mo–O–Mo and Mo–O–Zn bond angles around this oxygen atom is 356°). The unhybridized p orbital remaining on this oxygen atom is in excellent alignment to overlap with one d orbital on each of the adjacent Mo atoms in the trinuclear cluster. These d orbitals are the same ones that give rise to the nonbonding a_1 LUMO. The Mo–O π interaction would destabilize this a_1 orbital, making it antibonding in character. The same oxygen atoms in $LiZn_2Mo_3O_8$ and $Zn_3Mo_3O_8$ are each bonded to two Mo atoms and two Zn ions (or Li^+ ions in $LiZn_2Mo_3O_8$) in an arrangement that is halfway between an sp^2- and sp^3-like configuration. If the hybridization of this oxygen atom had remained essentially sp^2 planar, a weaker Mo–O π interaction would have been expected due to an increase in electron density resulting from the addition of the seventh or eighth electrons to the triangular clusters. In $LiZn_2Mo_3O_8$, the π overlap is further weakened because all of the oxygen atom's p orbitals are utilized in forming metal–oxygen bonds. The a_1 antibonding orbital is, therefore, lowered in energy but still possesses antibonding character. The seventh electron in the $LiZn_2Mo_3O_8$ clusters thus occupies this orbital and causes an increase in the Mo–Mo bond distance. The π interactions in the $Zn_3Mo_3O_8$ clusters are much weaker than in $LiZn_2Mo_3O_8$ for the reasons given above. This can be seen in the Mo1–O2 bond distance of 2.056 Å for $Zn_3Mo_3O_8$, which is rather long for an important contribution from π overlap. The antibonding a_1 orbital is lowered further in energy so as to become a weakly antibonding level. The seventh and eighth electrons in the $Zn_3Mo_3O_8$ clusters fill this orbital and cause essentially no change in the Mo–Mo bond length from that in $LiZn_2Mo_3O_8$.

It can be argued that the placement of zinc ion (Zn4) in a position that interacts with the otherwise nonhybridized p orbital on an oxygen atom (O2) causes the weakening of Mo–O π bonding. It can also be argued that the weakening of the Mo–O π bonding, due to electronic charge buildup on the clusters, allows zinc ion (Zn4) to occupy this otherwise nonavailable site. The true picture probably represents a synergistic effect between these two types of interactions. The assessment of Mo–O π vs. Zn–O interactions could possibly be clarified with a crystal structure determination of $ScZnMo_3O_8$. This compound, which is isostructural with $Zn_2Mo_3O_8$, would contain the sp^2-like planar oxygen atoms (O2); therefore, the effect of another cation competing for the lone-pair orbital on oxygen would be eliminated. Finally, we suggest that removal or reduction of the π-bonding capability of the edge-bridging atoms may be important to synthesis of stable seven- and eight-electron derivatives. In this connection we note that the reduction of $[Mo_3O_4(H_2O)_9]^{4+}$ in aqueous acid is accompanied by protonation of the bridging O atoms, as evidenced by the $[H^+]$ dependence of the half-wave potentials.[31]

Acknowledgment. We thank Professor Alfred P. Sattelberger for measurement of the magnetic susceptibility of $LiZn_2Mo_3O_8$ at room temperature and William W. Beers for the measurements over the range 94–300 K. The continuing support of this work by the U.S. Department of Energy, Basic Energy Sciences, is gratefully acknowledged.

Registry No. $LiZn_2Mo_3O_8$, 78402-82-1; $ScZnMo_3O_8$, 85255-50-1; $Zn_3Mo_3O_8$, 85255-51-2.

Supplementary Material Available: Tables of anisotropic temperature factors and structure factor amplitudes for $LiZn_2Mo_3O_8$ and $Zn_3Mo_3O_8$ and calculated and observed *d* spacings and relative intensities of X-ray powder diffraction reflections for $ScZnMo_3O_8$ and $Zn_3Mo_3O_8$ (12 pages). Ordering information is given on any current masthead page.

(30) Bursten, B. E.; Cotton, F. A.; Hall, M. B.; Najjar, R. C. *Inorg. Chem.* **1982**, *21*, 302.

(31) Richens, D. T.; Sykes, A. G. *Inorg. Chem.* **1982**, *21*, 418.